Title
Effects of silica-coated carbon nanotubes on the curing behavior and properties of epoxy composites

Journal
RSC Advances, 6(28)

ISSN
2046-2069

Authors
Li, Ao
Li, Weizhen
Ling, Yang
et al.

Publication Date
2016

DOI
10.1039/c5ra25182f

Peer reviewed

Effects of Silica-coated Carbon Nanotubes on the Curing Behavior and Properties of Epoxy Composites

[1] Ao Li, Weizhen Li*, Zonglian Xia, Yang Ling, Baoyu Wang, Wenjun Gan*

College of Chemistry and Chemical Engineering, Shanghai University of Engineering Science, 333 Longteng Road, Shanghai, 201620, China

[2] Michael A. Brady, Cheng Wang

Advanced Light Source, Lawrence Berkeley National Laboratory, 1 Cyclotron Road, Berkeley, CA 94720, USA

Corresponding author: Tel.: +86 21 67791217; fax: +86 21 67791214.

E-mail address: liwenzhen@sues.edu.cn, wjgan@sues.edu.cn

Abstract: Multi-walled carbon nanotubes (MWCNTs) were coated with silica by a sol-gel method to improve interfacial bonding and dispersion of nanotubes in diglycidyl ether of bisphenol A (DGEBA) matrix. TEM and FE-SEM measurements

showed that the silica shell had been successfully coated on the surface of r-MWCNTs (as received MWCNTs), and that the dispersion of MWCNT@SiO_2 in the epoxy matrix and interfacial adhesion between MWCNTs and epoxy were improved through the silica shell deposition. The effects of silica-coated multi-walled carbon nanotubes (MWCNT@SiO_2) on the curing behavior of epoxy resin, and on the physical and mechanical properties of epoxy composites, were studied. FT-IR measurements of different blends at different curing times indicated that the curing reaction was accelerated with the presence of MWCNTs and increased with the content of MWCNT@SiO_2. DSC results confirmed that the value of activation energy decreased with the introduction of MWCNTs in the order of MWCNT@SiO_2 < r-MWCNTs < epoxy. It was found that the mechanical properties and thermal conductivity of epoxy composites were significantly enhanced by incorporation of MWCNT@SiO_2, relative to composites with r-MWCNTs, while the values of glass transition temperature slightly increased, and the high electrical resistivity of these composites was retained overall.

Keywords: Silica-coated multi-walled carbon nanotube, Epoxy composite, Curing behavior, Physical and mechanical properties

1. Introduction

Carbon nanotubes (CNTs), discovered in 1991 by Iijima [[Iijima, 1991, HELICAL MICROTUBULES OF GRAPHITIC CARBON]1], are often referred to as one-dimensional materials because of their high aspect ratio and have excellent mechanical properties, such as high elastic modulus and high tensile strength. They

are considered to be the most promising reinforcement fillers for polymer matrices in improving their mechanical properties [2-5]. Meanwhile, CNTs have unusually high electrical and thermal conductivity [2-4,6-7] due to out-of-plane delocalized π electrons, σ - π rehybridization [2], and phonon-dominated ballistic heat transport [5,7-9].

As an important class of thermosetting polymers for high performance composites and electrical applications, epoxy resins show excellent electrical insulation properties, good chemical resistance, high adhesion, and low curing shrinkage. Incorporation of CNTs into epoxy resin has proven to be a good strategy for obtaining polymer composites with favorable mechanical properties [10-13], good thermal conductivity [14-18], and improved toughness [19-23].

Among the various polymer composites, epoxy-based systems are very important materials for electronic packaging applications. For such applications, thermally conducting but electrically insulating materials are required. The common advantage of CNTs being electrically conductive is no longer desired. A facile method for improving thermal conductivity while retaining high electrical resistivity is to incorporate silica-coated carbon nanotubes (CNTs@SiO_2) into the epoxy system [9,24-25]. Silica has been widely used as a filler in electronic packaging material. Silanized or silica-coated nanotubes can not only improve the interfacial adhesion between the CNTs and matrix and the resulting dispersion of CNTs in epoxy matrix,but also improve the composite's mechanical properties [25-27]. Although these studies showed a functional layer on the CNTs surface, providing a predicted reinforcement and improvement of thermal conductivity and electrical resistivity, the influence of the silica coating at the CNT surface on the curing behavior is still not well understood.

The incorporation of CNTs as reinforcement will surely enhance the mechanical and thermal properties of epoxy resins but would also modify their processing behavior. Characterization of the curing kinetics of the CNT-filled epoxy resin is one of the prerequisites for designing and optimizing the process parameters. Studies have been reported on the cure behaviors of CNT/epoxy [28-32] and surface treated-CNT/epoxy systems [33-38]. However, fewer reports exist regarding the effect of silica-coated CNTs on the curing behavior of epoxy composite resin.

Moreover, anhydride-cured epoxy resins will show improved properties over amine-cured resins, such as electrical insulation, low exotherms and shrinkage during curing, as well as low water absorption and almost internal stress-free systems after curing. Therefore, anhydride-cured systems are widely used as electrical insulation materials [39]. Although anhydride hardeners have been employed for CNT/epoxy composites [40-41], further study on the anhydride curing behavior is needed.

In this study, a simple sol-gel method was used to obtain silica-coated MWCNTs (MWCNT@SiO_2) directly from r-MWCNTs (as-received carboxylated MWCNTs), which was characterized by transmission electron microscopy (TEM). Anhydride-cured epoxy composites modified with r-MWCNTs (r-MWCNT/epoxy composites are used as an additional 'control' formulation, as no silica coating is present in these composites) and MWCNT@SiO_2 are then prepared and observed by scanning electron microscopy (SEM) and TEM. Subsequently, the curing process is monitored with Fourier transform infrared spectroscopy (FT-IR) and differential scanning calorimetry (DSC). The effects of various contents of r-MWCNTs and MWCNT@SiO_2 on the curing behavior will be discussed. Finally, the effects of various contents of r-MWCNTs and MWCNT@SiO_2 on the mechanical properties, electrical resistivity, and thermal conductivity are evaluated.

2. Experimental

2.1 Materials

Carboxylated MWCNTs, supplied from Shenzhen Nanotech Port Co. Ltd. with carboxylic groups on the surface, with a diameter of 20-40 nm and a length of 2-5 μm, were used as received (r-MWCNTs) directly because of their enhanced dispersibility. Tetraethylorthosilicate (TEOS), ethanol, ammonia and other chemical reagents were of analytical grade and supplied from Shanghai Reagents Co., China.

A commercial epoxy resin (DER 331, with an epoxide equivalent weight of 182-192) from Dow Chemical and a curing agent methyltetrahydrophthalic anhydride (MTHPA) and accelerator benzyldimethylamine (BDMA) from Shanghai TCI Chemical Industry Co. Ltd. were used without further purification.

2.2 Synthesis of silica-coated MWCNTs (MWCNT@SiO_2)

MWCNT@SiO_2 was prepared by the sol-gel method. 100 mg r-MWCNTs were firstly ultrasonically dispersed into 30 mL of deionized water for 1 h. The above suspension was then added to 80 mL of ethanol and ultrasonicated for another 0.5 h to form a stable dispersion. Immediately, 2 mL of $NH_3 \cdot H_2O$ was added into the as-prepared MWCNTs dispersion. Next, a TEOS solution (1 mL of TEOS in 40 mL of ethanol) was dropped into the MWCNT dispersion under mechanical stirring, and the mixture was stirred for another 12 h at room temperature to complete the reaction. Finally, the mixture was centrifuged and washed with ethanol repeatedly to remove the free silica particles. These processes were expected to result in the formation of a uniform and thick layer of silica on every individual MWCNT. The synthetic process of MWCNT@SiO_2 is presented in Scheme 1.

2.3 Preparation of MWCNTs/epoxy composites

MWCNT@SiO_2 (0.75, 1.5 and 2 wt% of epoxy composite) was dispersed in THF for 30 min by means of ultrasonication at room temperature. The obtained dispersion was then added to the preheated epoxy resin (60 °C) under ultrasonic vibration. Afterwards, the temperature was increased to 80 °C, and the mixture was ultrasonicated for another 1 h, followed by intensive mechanical stirring for 1 h to ensure homogeneity and allow the THF to evaporate. The curing agent Me-THPA was then added at an epoxy-to-hardener ratio of 1:0.8 by weight, and the mixture was degassed under vacuum to remove any trapped air bubbles. Finally, the mixture was cast in aluminum molds and cured at 80 °C for 30 min, followed by curing at 150 °C for another 5 h. Control samples of neat epoxy resin and r-MWCNT/epoxy composites were also prepared by the same procedure and conditions.

2.4 Characterization and Measurement

TEM images were taken on a JEOL-2100F microscope to characterize the r-MWCNTs and MWCNT@SiO_2. The morphological observations of the sample fracture surface were carried out by a field emission SEM (FESEM) (Hitachi Su-8010). The cryogenically fractured surfaces of the specimens were coated with platinum prior to their microscopy characterization.

The FT-IR spectra of r-MWCNTs, MWCNT@SiO_2, and composites modified with MWCNTs were recorded on a Nicolet AVATAR (Thermo Fisher, USA) with a resolution of 4 cm^{-1}. The curing behavior of the epoxy resin with and without MWCNTs was studied by isothermal FT-IR at 150 °C and nonisothermal DSC, using a PT-10 (Linseis, Germany) differential thermal analyzer at various heating rates of

2.5, 5, 10, 15 and 20 K/min, in the range of 30-300 °C, under nitrogen atmosphere.

A Servo-controlled tension tester CZ-8000 (Zhongzhi Testing Instruments, China) was used for tensile testing at a crosshead speed of 2 mm/min. Bulk electrical resistivity measurements were conducted using a plate electrode, type ZC36, high resistance meter (Shanghai Cany Precision Instrument Co., China). Thermal conductivity of the composites was measured at room temperature using a transient QTM-D2 heat-flow meter (SDK Co., Japan). Thermomechanical properties of the composites were evaluated by dynamic mechanical analysis (DMA) (TA Q800, USA) with a three-point bending mode. The heating rate was 3 °C/min in a temperature range of 30-250 °C, at a frequency of 1 Hz.

3. Results and Discussion

3.1 Carbon nanotube characterization

3.1.1 FT-IR analysis

FT-IR spectra for r-MWCNTs and MWCNT@SiO_2 are shown in Fig. 1. Carboxylic acid functional groups (-COOH) can be identified on the surface of the r-MWCNTs and MWCNT@SiO_2 by FT-IR spectroscopy. Vibrational modes at 3425/3417 and 1728/1718 cm^{-1} can be attributed to O-H stretching and carbonyl stretching of the carboxylic acid groups [26-27,42], respectively. The spectra show that a certain amount of carboxylic acid groups are attached to both r-MWCNTs and MWCNT@SiO_2. Compared with r-MWCNTs, new obvious peaks at 2922 and 2852 cm^{-1} are observed, which can be attributed to C-H stretching and bending modes from the TEOS molecules, for MWCNT@SiO_2. Furthermore, the absorbance peaks at 1065, 964 and 793 cm^{-1} are also observed, which are responding to the Si-O-Si

stretching and bending modes and the stretching of Si-OH groups, respectively, for the hydroxylated silica-coated nanotubes [26,27]. These new peaks suggest that the r-MWCNTs were indeed modified by the silica deposition.

3.1.2 Morphology

The morphology of synthesized MWCNT@SiO_2 was studied using TEM, and the images are shown in Fig. 2. No obvious silica particles can be observed, and the entanglement between the tubes appears to be weak. The core/shell structure of MWCNT@SiO_2, with insulating silica as the shell and MWCNT as the core, can be observed in Fig. 2b. The diameters of the tubes are uniform, with an average value of approximately 90 nm, while the length of the tubes is on the order of several micrometers. Thus, TEM indicates that a silica shell of approximately 30 nm thickness (20-40 nm diameter for r-MWCNTs) was successfully coated on the r-MWCNTs by the sol-gel process, and that the silica detected by FT-IR indeed exists as a coating on the outside surface of r-MWCNTs.

3.2 Composite characterization

3.2.1 Morphology of fracture surface

In order to investigate the dispersibility and the interfacial adhesion of MWCNTs in the epoxy matrix, the prepared epoxy composites were cryogenically fractured, and the morphology of the cross section was examined. Fig. 3 presents the representative SEM images of the fractured surfaces for the composites with 2.0 wt% of r-MWCNTs and MWCNT@SiO_2.

Good dispersion of r-MWCNTs in the epoxy matrix can be seen in Fig. 3. There are only a few visible r-MWCNTs, highlighted by yellow circles, that were not incorporated in the epoxy matrix. Fig. 3 indicates that r-MWCNTs are generally embedded in the epoxy matrix, and the interfacial adhesion between MWCNTs and epoxy are improved through the carboxylic acid surface chemistry of r-MWCNTs.

By comparison, the MWCNT@SiO_2/epoxy composite shows improved dispersion and homogeneity on the fractured surface (Fig. 3). Most of the MWCNT@SiO_2 are embedded in the epoxy matrix, and fewer of them are spatially separated from the matrix as compared to the r-MWCNT/epoxy composite, suggesting that stronger interfacial bonding exists between epoxide/hydroxyl groups in the epoxy matrix and carbonyl/carboxylic groups on MWCNT@SiO_2. Consequently, the compatibility and interfacial adhesion between MWCNT@SiO_2 and epoxy are improved through the silica coating of r-MWCNT. As interpreted by Cui [9], another reason for this may be due to the uniform silica shell serving as an intermediate layer between the MWCNT and the epoxy matrix, minimizing tube-tube aggregation.

3.3 Curing behavior of composites

3.3.1 Isothermal FT-IR analysis

The effect of the silica layer on the MWCNT surface on the curing behavior of epoxy composites is quite important for the final properties of the composite. Here, FT-IR is used to investigate the curing reaction rate of neat epoxy and MWCNT/epoxy composites. Fig. 4(a) and (b) show the FT-IR spectra of the neat epoxy and epoxy composites cured at 150 °C at different times.

In both systems, the characteristic stretching features of epoxy groups at 915 cm^{-1}

and 923 cm^{-1} decrease in intensity gradually; the signatures of the anhydride group at X cm^{-1} and carboxylic acid group at 1844 cm^{-1} decrease quickly with reaction time from the beginning of the reaction until 60 min. Peaks at 1606, 1581, 1508 and 1456 cm^{-1} originate from bond stretching of the benzene ring from MWCNT?. The extent of reaction (α) can be calculated by the disappearance of the characteristic peak of the epoxy group at 915 cm^{-1}, with the stretching vibration peak of benzene at 1606 cm^{-1} chosen as the reference peak [34-35]:

(1)

From Fig. 4c and 4d, it can be seen that the reaction rate curves are typically autocatalytic, with maximum rates of reaction occurring immediately after the start of the reaction [29]. From Fig. 4c, it is found that the curing reaction rate of each epoxy composite is faster than the neat epoxy resin. Moreover, when the r-MWCNTs were coated with silica, the curing reaction conversion and rate are increased significantly. It is believed that the -OH groups on the surface of silica-coated MWCNTs exert a catalytic effect for epoxide ring opening [29].

Furthermore, the initial reaction rates are affected by the presence and concentration of r-MWNTs and MWCNT@SiO_2, increasing as the MWCNT@SiO_2 content increases, as shown in Figure 4(d). The influence of MWCNT@SiO_2 on the curing reaction absolute conversion and rate is significant, relative to the curing reaction of neat epoxy resin and the r-MWCNT-filled epoxy resin. This can be explained by the consideration of hydroxyl groups at the silica surface, induced by the sol-gel process, that hydrogen bond with the epoxide ring and act as an accelerant to increase the curing reaction rate. As the MWCNT@SiO_2 content is increased, the larger content of surface hydroxyl groups available for hydrogen bonding will lead to

an increased conversion rate.

3.3.2 DSC analysis

DSC measurements were also carried out to further study the effect of the silica coating on the composites' curing behavior. Fig. 5(a) presents DSC curves of neat epoxy and epoxy composites at a heating rate of 10 °C/min. The peak maximum temperatures (T_p) of the epoxy curing reactions are summarized in Table 1.

At a certain heating rate, the peak temperature of the exothermic curve decreased when r-MWCNTs or MWCNT@SiO_2 are added, and this phenomenon indicated that -OH groups on the surface of MWCNTs might accelerate the curing reaction, which is consistent with the results of FT-IR.

A plot of $\ln(\beta/T_p^2)$ versus $1000/T_p$, according to the Kissinger equation [43](2), allows the determination of the curing reaction activation energy, which is shown in Figure 5(b).

(2)

where β is a constant heating rate, E_a is the activation energy, and R is the gas constant (8.314J mol^{-1} K^{-1}).

The activation energy calculated for neat epoxy, r-MWCNT/epoxy (1.5 wt%) and MWCNT@SiO_2/epoxy (1.5 wt%) composites are 77.3 kJ/mol, 71.2 kJ/mol and 62.7 kJ/mol, respectively. This indicates that the introduction of MWCNTs decreases the activation energy of the curing reaction. This decrease of the activation energy may be explained by the consideration that the carbonyl/carboxyl? groups on the r-MWCNT surface and the hydroxyl groups enriched on the MWCNT@SiO_2 surface form a hydrogen bond with the oxirane ring, which decreases the energy barrier of curing reaction and accelerates the cross-linking reaction. This result is consistent with the

results from FT-IR measurements. As expected, the effect of the presence of hydroxyl groups on decreasing the activation energy is more obvious than that of the carbonyl group. As suggested by Lavorgna *et al.*, some reactive groups present in the silica-coated nanotubes such as SiOH groups may catalyze the epoxy crosslinking reactions [26].

3.4 Physical and mechanical properties of epoxy composites

3.4.1 Electrical resistivity

MWCNTs are widely used to improve the electrical conductivity of industrial composites. However, electrical insulation is required for the electronic packaging applications discussed in this report. Herein, silica was coated on the surface of r-MWCNTs, and the effect of different MWCNT concentrations on the electrical resistivity of the epoxy composites was studied, and the results are shown in Fig. 6. The electrical resistivity of the epoxy composites with 1.5 wt% r-MWCNTs decreases sharply by three orders of magnitude, with respect to the neat epoxy, from 2.3×10^{-15} to 1.9×10^{-12} Ω cm, while the electrical resistivity of the epoxy composites with the same content of MWCNT@SiO_2 exhibits a smaller decrease relative to neat epoxy, from 2.3×10^{-15} to 3.1×10^{-13} Ω cm. Specifically for the MWCNT@SiO_2 concentration range from 0.75 to 1.5 wt%, the value of electrical resistivity is nearly constant.

When the concentration of r-MWCNTs is increased to 2.0 wt%, the dispersion morphology becomes coarsened due to nanotube aggregation, the electrically conductive network is broken, and the electrical resistivity increases again partially. For the MWCNT@SiO_2/epoxy composites, the electrical resistivity remains nearly constant once the nanotube concentration exceeds 0.75 wt%. The difference between the two composites' electrical resistivity behavior is explained by the consideration

that the silica shell for MWCNT@SiO_2/epoxy composites can prevent MWCNTs from coming into physical contact and aggregating, therefore resulting in a less interconnecting network that effectively blocks the electron movement between MWCNTs [9].

3.4.2 Thermal conductivity

The highest reported nanotube thermal conductivities are on the order of 10^3 W/(m K), while typical polymers have κ~ 0.1 W/(m K). For an application of epoxy in electronic packaging, the excellent thermal conductivity of nanotubes leads to early expectations that it will enhance the thermal conductivity of epoxy nanocomposites [4]. Fig. 7 shows that the dispersion of 0.75, 1.5 and 2.0 wt% MWCNTs into epoxy resin does indeed increase the thermal conductivity. In addition, the thermal conductivity of epoxy composites increases as the content of MWCNTs increases. Interestingly, the r-MWCNT composites exhibit a smaller enhancement than MWCNTs@SiO_2 in spite of the low thermal conductivity of the amorphous silica coating. For the r-MWCNT/epoxy composites, the thermal conductivity increases by 63.6% from 0.11 for neat epoxy resin to 0.18 W/mk at 2.0 wt% of r-MWCNTs. For the MWCNT@SiO_2/epoxy composites, a significant improvement in the thermal conductivity of 127% from 0.11 to 0.25 W/mk was observed.

Phonons entering the MWCNT/epoxy composite are much more likely to travel through the matrix than electrons because the contrast in thermal conductivity ($\kappa_{nanotube}/\kappa_{polymer}$) is ~$10^4$ in comparison to the electrical conductivity contrast ($\sigma_{nanotube}/\sigma_{polymer}$) of ~$10^{15}$-$10^{19}$ [4]. Therefore, the difference in thermal conductivity between r-MWCNT/epoxy and MWCNT@SiO_2/epoxy composites indicates that the silica shell both improves the interfacial heat transport between the epoxy matrix and

the MWCNT@SiO_2 and leads to better dispersion of MWCNT@SiO_2 in the epoxy matrix, implying that the improved interfacial adhesion and heat transport are both factors leading to the enhanced thermal conductivity for epoxy composites containing silica-coated MWCNTs.

3.4.3 Thermomechanical properties

The improved interfacial interactions between the functionalized MWCNTs and epoxy matrix also result in enhancements of glassy and rubbery moduli for such composites [27]. The storage modulus (E') and the loss factor (tan δ) of neat epoxy and epoxy composites with different MWCNTs at a concentration of 0.75 wt% are shown in Fig. 8. It is found that the incorporation of MWCNTs into the epoxy system results in an increase in storage modulus E', and the E' of samples increases gradually in the order of neat epoxy, r-MWCNT/epoxy, and MWCNT@SiO_2/epoxy composites in the glassy plateau region. This trend may be explained by the contribution of the hydroxyl groups, at the silica surface, to the improvement of both the compatibility of the filler with the epoxy matrix and the more effective dispersion of MWCNT@SiO_2 in the epoxy matrix.

The rubbery plateau of the storage modulus can be used as an indication of the degree of interaction between the epoxy matrix and the MWCNT fillers. At the content of 0.75 wt%, the rubbery modulus for the epoxy composites is ~12 MPa, while that for the neat epoxy is ~0 MPa. This enhancement in the rubbery modulus is directly correlated to the improvement in the interfacial interactions of MWCNT/epoxy composites.

The glass transition temperature (T_g) is closely linked to the thermomechanical stability and is thus a critical property that dictates the potential application of a given

epoxy resin [31]. The tan δ, equal to the ratio of the loss modulus to the storage modulus, as a function of the temperature, for neat epoxy and composites with 0.75 wt% of MWCNTs is presented in Fig. 8b. The T_g is obtained from the peak maximum position of the temperature-dependent tan δ curve. The T_g of r-MWCNT/epoxy and MWCNT@SiO_2/epoxy composites shifts to a slightly higher temperature, with the MWCNT@SiO_2/epoxy composites exhibit the highest glass transition temperature. This result agrees with literature reports [9,24,26-27]. The addition of MWCNT@SiO_2 in the epoxy resin increases T_g to 111 °C from 104 °C for neat epoxy, compared with the increase in T_g to 107 °C for r-MWCNT/epoxy composites. This difference in the glass transition is the result of the strong interaction between the hydroxyl groups enriched on silica shell of MWCNT@SiO_2 and the epoxy matrix, therefore enhancing the interfacial adhesion and restricting the segmental motion of the epoxy chains under shear. This finding is also in agreement with the accelerated curing reach observed for composites containing silica-functionalized MWCNTs from FT-IR and DSC results.

3.4.4 Tensile behavior

Fig. 9a shows the tensile elastic moduli of the epoxy composites with different contents of r-MWCNT or MWCNT@SiO_2. Compared with the neat epoxy, the elastic moduli for r-MWCNT/epoxy and MWCNT@SiO_2/epoxy composites at 1.5 wt% of MWCNTs increased by 41% and 88%, respectively. This significant improvement for the MWCNT@SiO_2/epoxy composite is due to the superior compatibility between the epoxy matrix and MWCNT@SiO_2 filler. As the filler concentration is increased, MWCNTs are increasingly able to aggregate, and thus the tensile strength begins to decline when the MWCNT concentration reaches 2.0 wt%. Aggregated MWCNTs

will lead to a reduction in the MWCNT-epoxy interfacial area and thus a reduction in the favorable interfacial adhesion, resulting in a reduced crack propagation energy in the matrix. This trend is in agreement with the results reported by Jia [41].

As shown in Fig. 9b, the elastic modulus of different composites presents the same tendency with the tensile strength. The elastic modulus of epoxy composites achieve maximum values at MWCNTs content of 1.5 wt% and decline at 2.0 wt% due to agglomeration of MWCNTs.

4. Conclusions

A uniform silica shell was successfully coated on the surface of MWCNTs by a sol-gel process, and the MWCNT@SiO_2 was incorporated into an epoxy matrix as filler. The effects of silica-functionalized MWCNTs on the curing behavior, electrical and thermal conductivity, and mechanical properties of epoxy-based composites were studied. The results highlight that the curing reaction increased with the introduction of r-MWCNTs and MWCNT@SiO_2, while the activation energy decreased. The silica shell of the functionalized MWCNTs improved the interfacial bonding and resulted in a better dispersion of MWCNTs in the matrix. Meanwhile, the mechanical properties and thermal conductivity were improved significantly by introduction of MWCNT@SiO_2 into epoxy resin. Moreover, the MWCNT@SiO_2/epoxy composites kept the higher electrical resistivity simultaneously. Therefore, the systematic study of the incorporation of functionalized MWCNTs, as a function of composite concentration, on the curing behavior, electrical and thermal conductivity, and mechanical properties presented here provides a processing window for obtaining each optimized property that is needed in electronic packaging applications.

Acknowledgments

The authors wish to thank the Shanghai Municipal Education Commission (Overseas Visiting Scholar Project 20120407); Shanghai Young Teachers' Training-funded Projects (ZZGJD13018); Shanghai University of Engineering Science Developing funding (grant 2011XZ04), start-up project funding (grant 0501-13-018) and Interdisciplinary Subject Construction funding (grant 2012SCX005).

References

X[1] Iijima S. HELICAL MICROTUBULES OF GRAPHITIC CARBON. Nature. 1991;354(6348):56-8.
[2] Dervishi E, Li ZR, Xu Y, Saini V, Biris AR, Lupu D, et al. Carbon Nanotubes: Synthesis, Properties, and Applications. Particulate Science and Technology. 2009;27(2):107-25.
[3] Ma PC, Siddiqui NA, Marom G, Kim JK. Dispersion and functionalization of carbon nanotubes for polymer-based nanocomposites: A review. Composites Part a-Applied Science and Manufacturing. 2010;41(10):1345-67.
[4] Moniruzzaman M, Winey KI. Polymer nanocomposites containing carbon nanotubes. Macromolecules. 2006;39(16):5194-205.
[5] Coleman JN, Khan U, Blau WJ, Gun'ko YK. Small but strong: A review of the mechanical properties of carbon nanotube-polymer composites. Carbon. 2006;44(9):1624-52.
[6] Berber S, Kwon YK, Tomanek D. Unusually high thermal conductivity of carbon nanotubes. Physical Review Letters. 2000;84(20):4613-6.
[7] Kim P, Shi L, Majumdar A, McEuen PL. Thermal transport measurements of individual multiwalled nanotubes. Physical Review Letters. 2001;87(21):4.
[8] Wang SR, Liang R, Wang B, Zhang C. Dispersion and thermal conductivity of carbon nanotube composites. Carbon. 2009;47(1):53-7.
[9] Cui W, Du FP, Zhao JC, Zhang W, Yang YK, Xie XL, et al. Improving thermal conductivity while retaining high electrical resistivity of epoxy composites by incorporating silica-coated multi-walled carbon nanotubes. Carbon. 2011;49(2):495-500.
[10] Allaoui A, Bai S, Cheng HM, Bai JB. Mechanical and electrical properties of a MWNT/epoxy composite. Composites Science and Technology. 2002;62(15):1993-8.
[11] Kim JA, Seong DG, Kang TJ, Youn JR. Effects of surface modification on rheological and mechanical properties of CNT/epoxy composites. Carbon. 2006;44(10):1898-905.
[12] Gojny FH, Schulte K. Functionalisation effect on the thermo-mechanical behaviour of multi-wall carbon nanotube/epoxy-compo sites. Composites Science and Technology. 2004;64(15):2303-8.
[13] Puglia D, Valentini L, Kenny JM. Analysis of the cure reaction of carbon nanotubes/epoxy resin composites through thermal analysis and Raman spectroscopy. Journal of Applied Polymer Science. 2003;88(2):452-8.

[14] Yang K, Gu MY, Guo YP, Pan XF, Mu GH. Effects of carbon nanotube functionalization on the mechanical and thermal properties of epoxy composites. Carbon. 2009;47(7):1723-37.
[15] Yang SY, Ma CCM, Teng CC, Huang YW, Liao SH, Huang YL, et al. Effect of functionalized carbon nanotubes on the thermal conductivity of epoxy composites. Carbon. 2010;48(3):592-603.
[16] Song YS, Youn JR. Influence of dispersion states of carbon nanotubes on physical properties of epoxy nanocomposites. Carbon. 2005;43(7):1378-85.
[17] Gojny FH, Wichmann MHG, Fiedler B, Kinloch IA, Bauhofer W, Windle AH, et al. Evaluation and identification of electrical and thermal conduction mechanisms in carbon nanotube/epoxy composites. Polymer. 2006;47(6):2036-45.
[18] Moisala A, Li Q, Kinloch IA, Windle AH. Thermal and electrical conductivity of single- and multi-walled carbon nanotube-epoxy composites. Composites Science and Technology. 2006;66(10):1285-8.
[19] Gojny FH, Wichmann MHG, Kopke U, Fiedler B, Schulte K. Carbon nanotube-reinforced epoxy-compo sites: enhanced stiffness and fracture toughness at low nanotube content. Composites Science and Technology. 2004;64(15):2363-71.
[20] Geng Y, Liu MY, Li J, Shi XM, Kim JK. Effects of surfactant treatment on mechanical and electrical properties of CNT/epoxy nanocomposites. Composites Part a-Applied Science and Manufacturing. 2008;39(12):1876-83.
[21] Kim MT, Rhee KY, Park SJ, Hui D. Effects of silane-modified carbon nanotubes on flexural and fracture behaviors of carbon nanotube-modified epoxy/basalt composites. Composites Part B-Engineering. 2012;43(5):2298-302.
[22] Tang LC, Wan YJ, Peng K, Pei YB, Wu LB, Chen LM, et al. Fracture toughness and electrical conductivity of epoxy composites filled with carbon nanotubes and spherical particles. Composites Part a-Applied Science and Manufacturing. 2013;45:95-101.
[23] Chung MH, Chen LM, Wang WH, Lai YS, Yang PF, Lin HP. Effects of mesoporous silica coated multi-wall carbon nanotubes on the mechanical and thermal properties of epoxy nanocomposites. Journal of the Taiwan Institute of Chemical Engineers. 2014;45(5):2813-9.
[24] Ma PC, Kim JK, Tang BZ. Effects of silane functionalization on the properties of carbon nanotube/epoxy nanocomposites. Composites Science and Technology. 2007;67(14):2965-72.
[25] Kathi J, Rhee KY, Lee JH. Effect of chemical functionalization of multi-walled carbon nanotubes with 3-aminopropyltriethoxysilane on mechanical and morphological properties of epoxy nanocomposites. Composites Part a-Applied Science and Manufacturing. 2009;40(6-7):800-9.
[26] Lavorgna M, Romeo V, Martone A, Zarrelli M, Giordano M, Buonocore GG, et al. Silanization and silica enrichment of multiwalled carbon nanotubes: Synergistic effects on the thermal-mechanical properties of epoxy nanocomposites. European Polymer Journal. 2013;49(2):428-38.
[27] Ma PC, Mo SY, Tang BZ, Kim JK. Dispersion, interfacial interaction and re-agglomeration of functionalized carbon nanotubes in epoxy composites. Carbon. 2010;48(6):1824-34.
[28] Xie HF, Liu BH, Yuan ZR, Shen JY, Cheng RS. Cure kinetics of carbon nanotube/tetrafunctional epoxy nanocomposites by isothermal differential scanning calorimetry. Journal of Polymer Science Part B-Polymer Physics. 2004;42(20):3701-12.
[29] Tao K, Yang SY, Grunlan JC, Kim YS, Dang BL, Deng YJ, et al. Effects of carbon nanotube fillers on the curing processes of epoxy resin-based composites. Journal of Applied Polymer Science. 2006;102(6):5248-54.
[30] Allaoui A, El Bounia N. How carbon nanotubes affect the cure kinetics and glass transition temperature of their epoxy composites? - A review. Express Polymer Letters. 2009;3(9):588-94.
[31] Zhou TL, Wang X, Liu XH, Xiong DS. Influence of multi-walled carbon nanotubes on the cure behavior of epoxy-imidazole system. Carbon. 2009;47(4):1112-8.
[32] Cui LJ, Wang YB, Xiu WJ, Wang WY, Xu LH, Xu XB, et al. Effect of functionalization of multi-walled carbon nanotube on the curing behavior and mechanical property of multi-walled carbon nanotube/epoxy composites. Materials & Design. 2013;49:279-84.
[33] Guadagno L, De Vivo B, Di Bartolomeo A, Lamberti P, Sorrentino A, Tucci V, et al. Effect of functionalization on the thermo-mechanical and electrical behavior of multi-wall carbon nanotube/epoxy composites. Carbon. 2011;49(6):1919-30.
[34] Yang K, Gu MY, Jin YP. Cure Behavior and Thermal Stability Analysis of Multiwalled Carbon Nanotube/Epoxy Resin Nanocomposites. Journal of Applied Polymer Science. 2008;110(5):2980-8.
[35] Yang K, Gu MY, Jin YP, Mu GH, Pan XF. Influence of surface treated multi-walled carbon nanotubes on cure behavior of epoxy nanocomposites. Composites Part a-Applied Science and Manufacturing. 2008;39(10):1670-8.

[36] Choi WJ, Poweii RL, Kim DS. Curing Behavior and Properties of Epoxy Nanocomposites With Amine Functionalized Multiwall Carbon Nanotubes. Polymer Composites. 2009;30(4):415-21.
[37] Wang F, Li SQ, Wang JW, Xiao J. Effect of functionalized multi-walled carbon nanotubes on the curing behavior and thermal stability of epoxy resin. High Performance Polymers. 2012;24(2):97-104.
[38] Rocks J, Rintoul L, Vohwinkel F, George G. The kinetics and mechanism of cure of an amino-glycidyl epoxy resin by a co-anhydride as studied by FT-Raman spectroscopy. Polymer. 2004;45(20):6799-811.
[39] Miyagawa H, Drzal LT. Thermo-physical and impact properties of epoxy nanocomposites reinforced by single-wall carbon nanotubes. Polymer. 2004;45(15):5163-70.
[40] Jia XL, Li G, Liu BY, Luo YM, Yang G, Yang XP. Multiscale reinforcement and interfacial strengthening on epoxy-based composites by silica nanoparticle-multiwalled carbon nanotube complex. Composites Part a-Applied Science and Manufacturing. 2013;48:101-9.

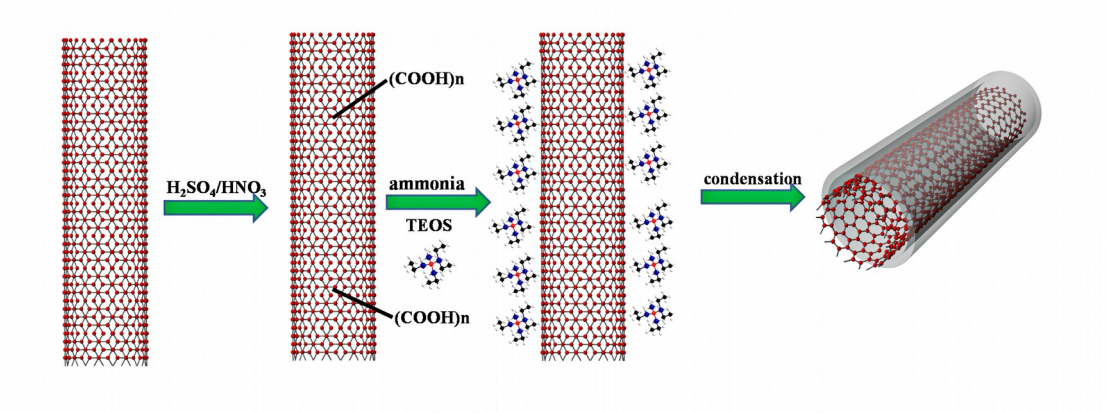

Scheme 1. The synthetic preparation of MWCNT@SiO_2.

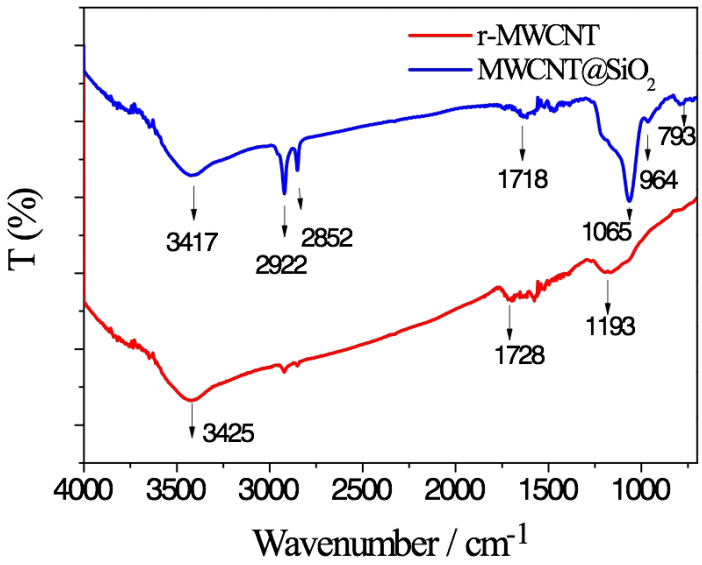

Fig. 1 FT-IR spectra of r-MWCNTs and MWCNT@SiO_2.

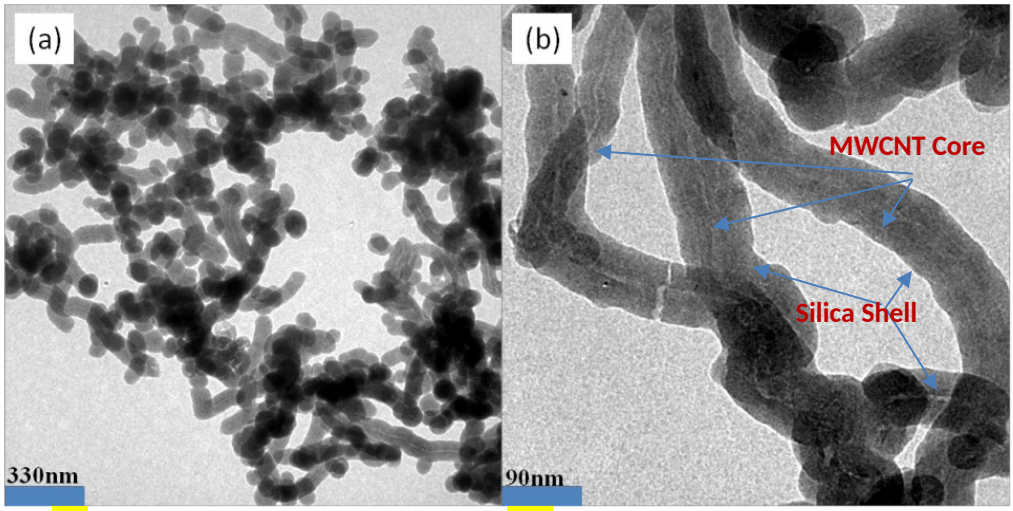

Fig. 2 (a) TEM image of MWCNT@SiO_2. (b) Higher magnification image of (a).

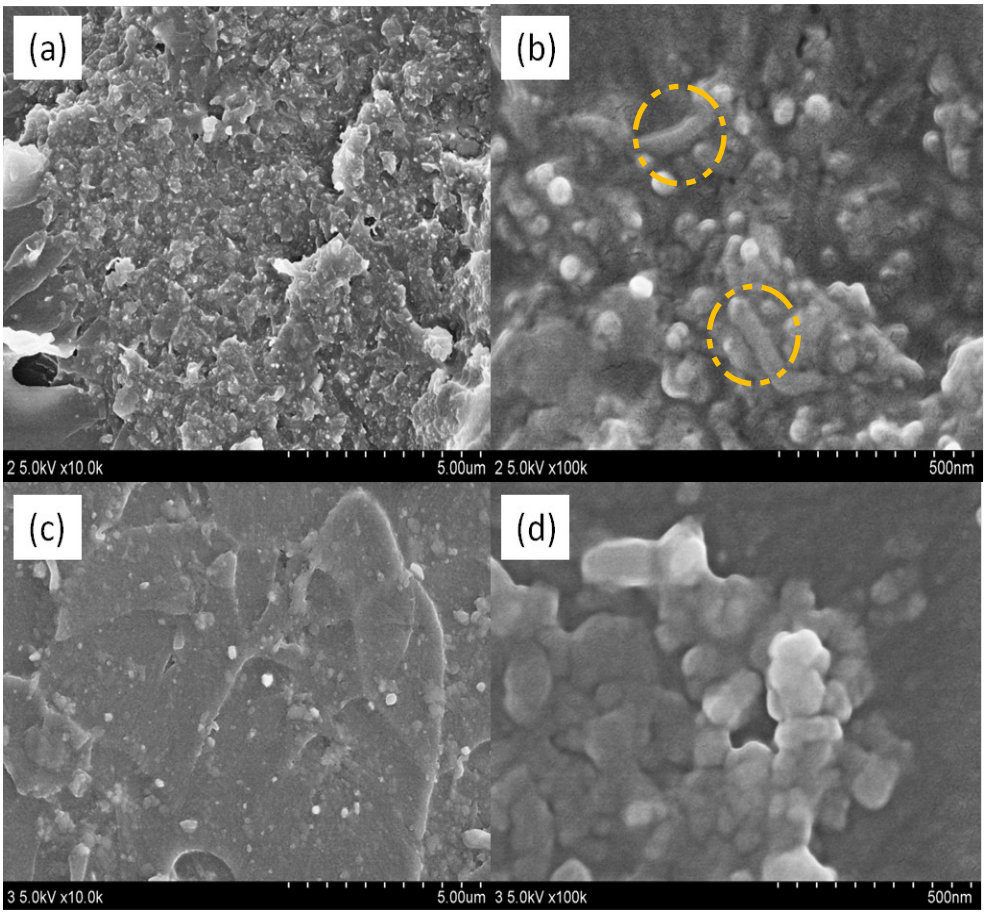

Fig. 3 FE-SEM images of the fracture surfaces for epoxy composites containing 2.0 wt% of (a,b) r-MWCNTs, (c,d) MWCNT@SiO_2. The yellow circles in (b) highlight nanotubes that have not been incorporated into the matrix.

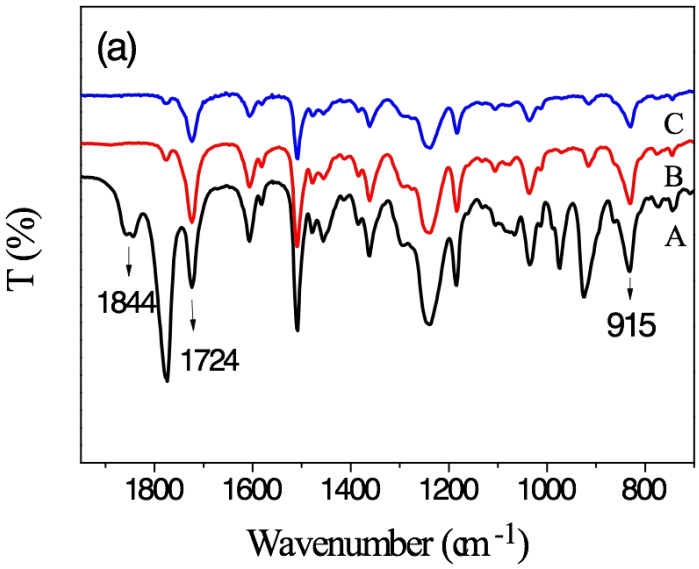
(a)
C
B
A
1844
1724
915
T (%)
1800
1600
1400
1200
1000
800
Wavenumber (cm-1)

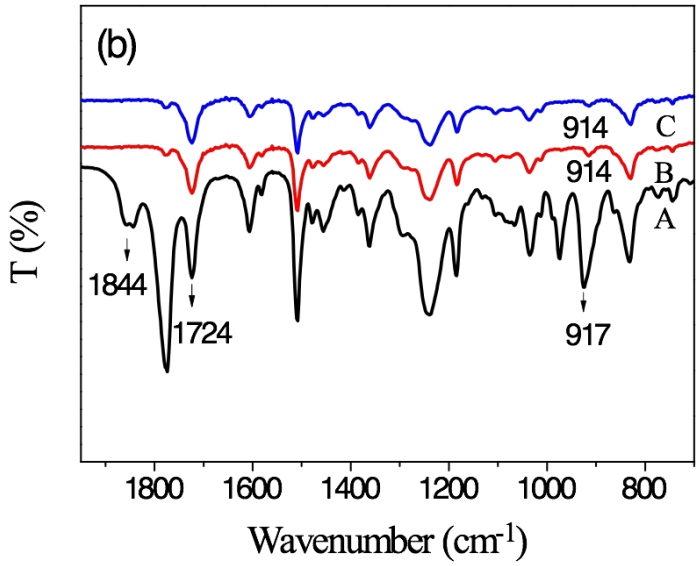
(b)
914
C
914
B
A
1844
1724
917
T (%)
1800
1600
1400
1200
1000
800
Wavenumber (cm-1)

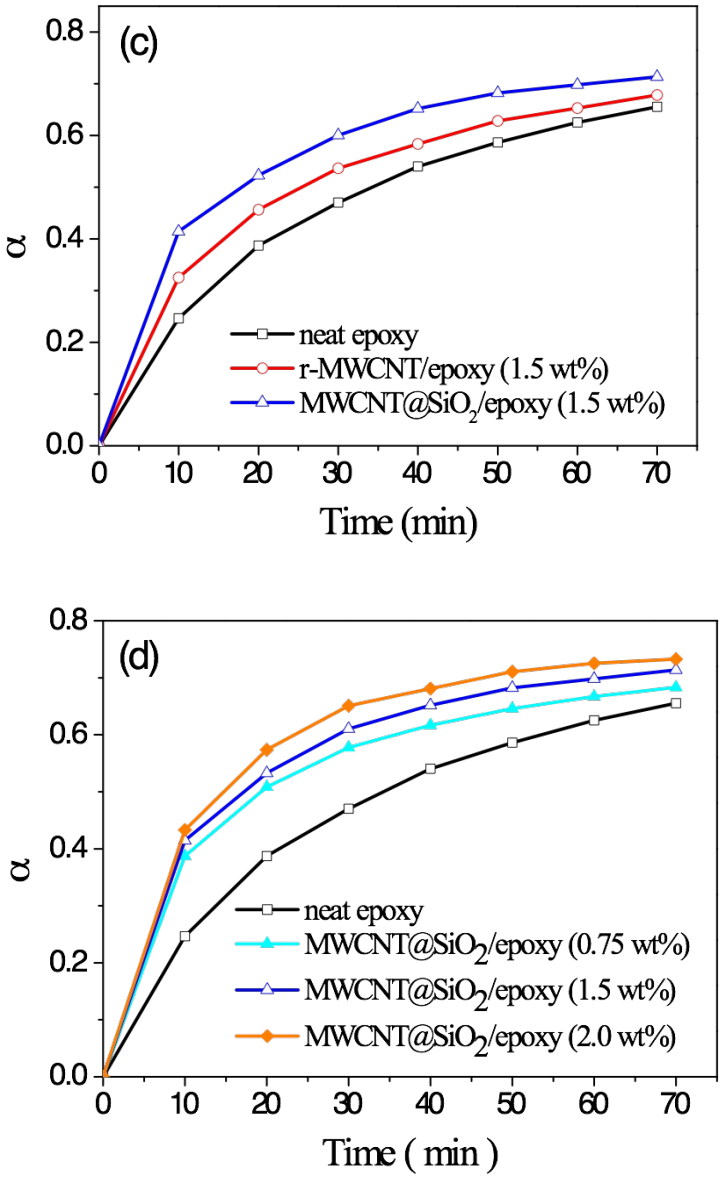

Fig. 4 FT-IR spectra of (a) neat epoxy and (b) MWCNT/epoxy composites, cured at 150 °C for (A) 0 min, (B) 30 min and (C) 60 min; (c) reaction conversion versus time for neat epoxy and epoxy composites cured at 150 °C and (d) for MWCNT@SiO_2/epoxy composites with different contents of MWCNT@SiO_2, cured at 150 °C.

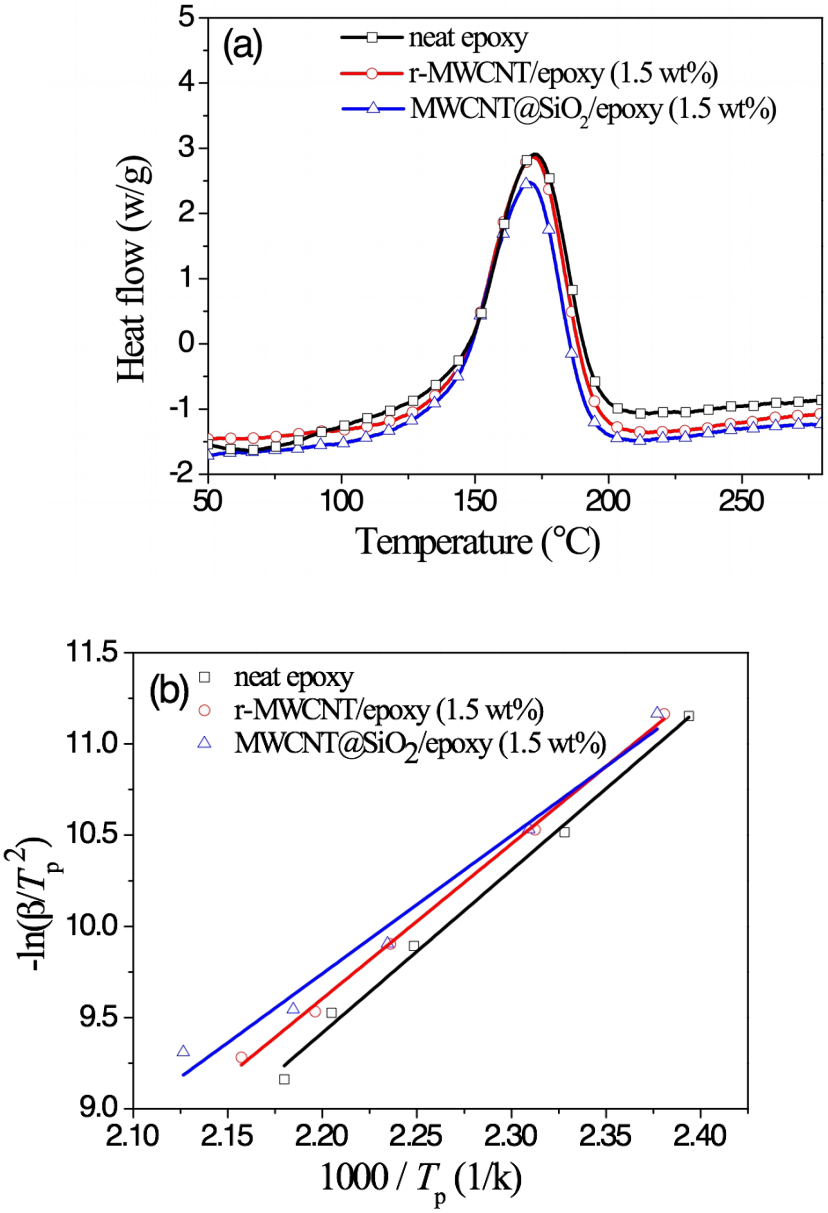

Fig. 5 (a) DSC curves of neat epoxy and epoxy composites at a heating rate of 10 °C/min; (b) Arrhenius behavior of epoxy curing based on the DSC results.

Table 1 T_p values (K) for epoxy and composites from the DSC measurement at different heating rates.

Material	T_p, 2.5 K/min	T_p, 5 K/min	T_p, 10 K/min	T_p, 15 K/min	T_p, 20 K/min
neat epoxy	419.2	432.5	445.4	453.7	458.5
r-MWCNTs/epoxy (1.5/100)	418.4	430.4	444.2	451.6	457.3
MWCNT@SiO2/epoxy(1.5/100)	416.5	429.4	442.1	448.5	455.4

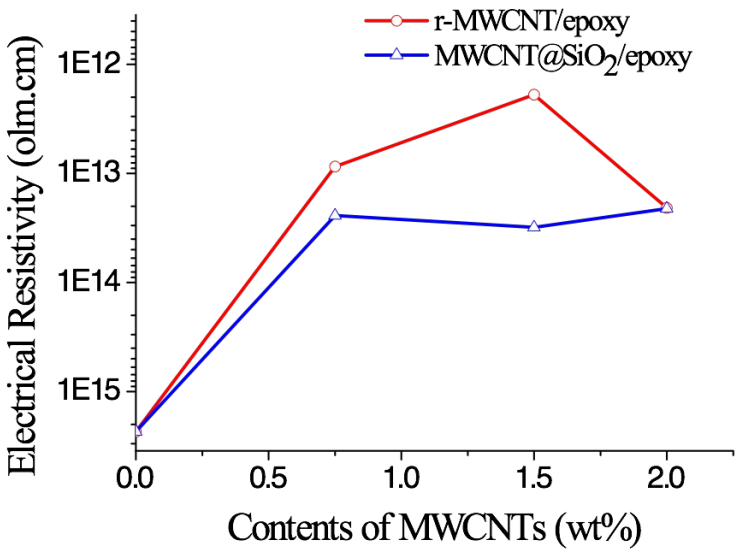

Fig. 6 Electrical resistivity for both MWCNT surface chemistries, as a function of MWCNT concentration, in epoxy composites.

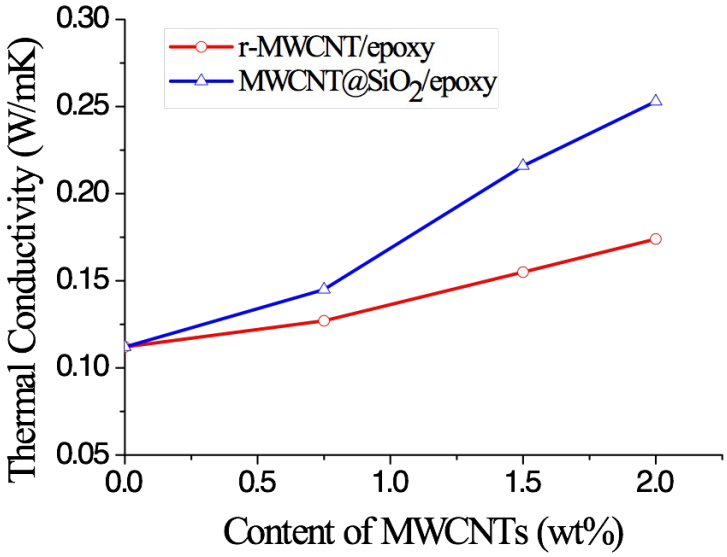

Fig. 7 Thermal conductivities for epoxy composites as a function of content of r-MWCNT and MWCNT@SiO_2 concentration.

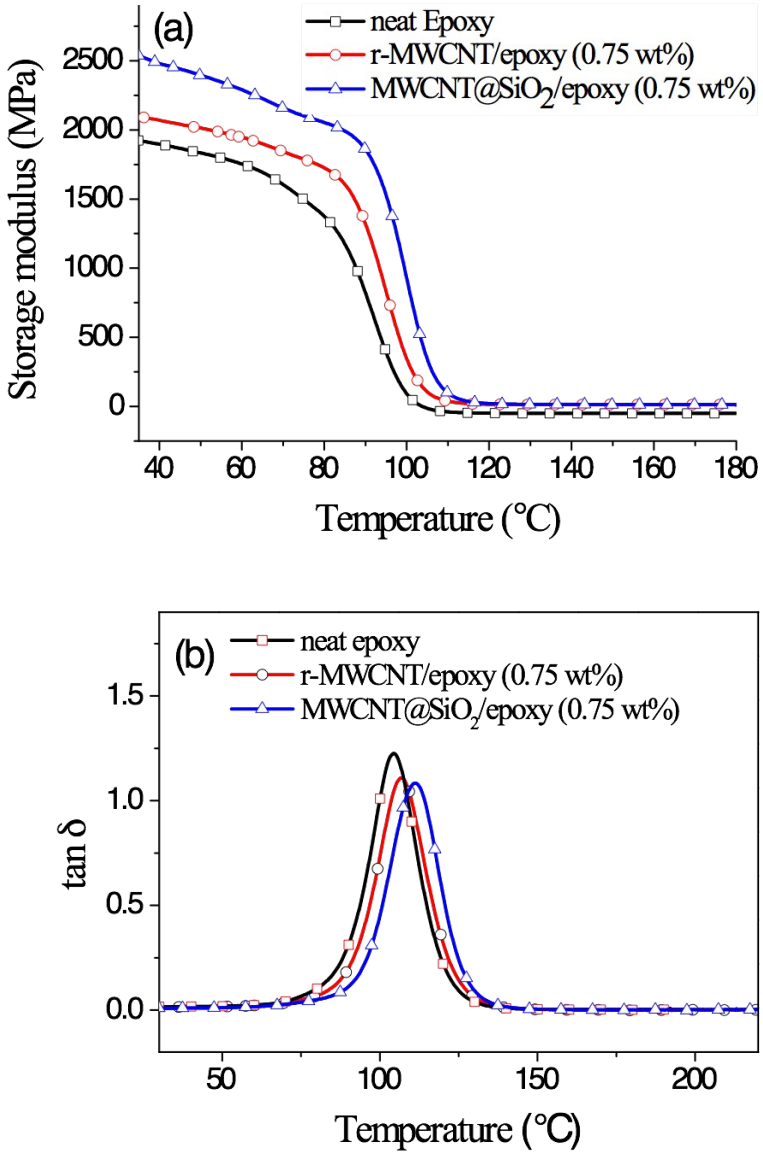

Fig. 8 (a) Storage modulus (E') and (b) loss factor (tan δ) of neat epoxy and epoxy composites with a concentration of 0.75 wt% of either r-MWCNT or MWCNT@SiO_2.

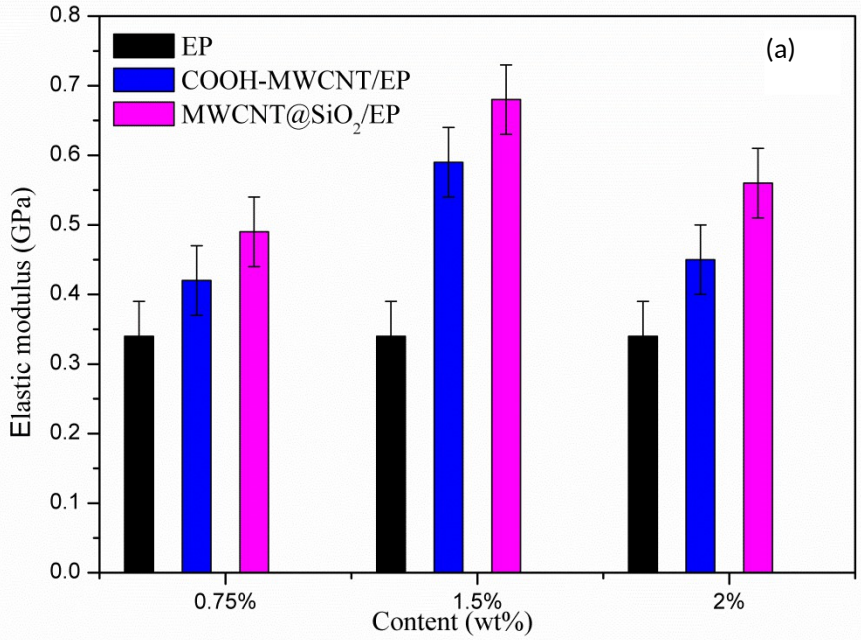
EP
COOH-MWCNT/EP
MWCNT@SiO2/EP
(a)
Elastic modulus (GPa)
0.0
0.1
0.2
0.3
0.4
0.5
0.6
0.7
0.8
0.75%
1.5%
2%
Content (wt%)

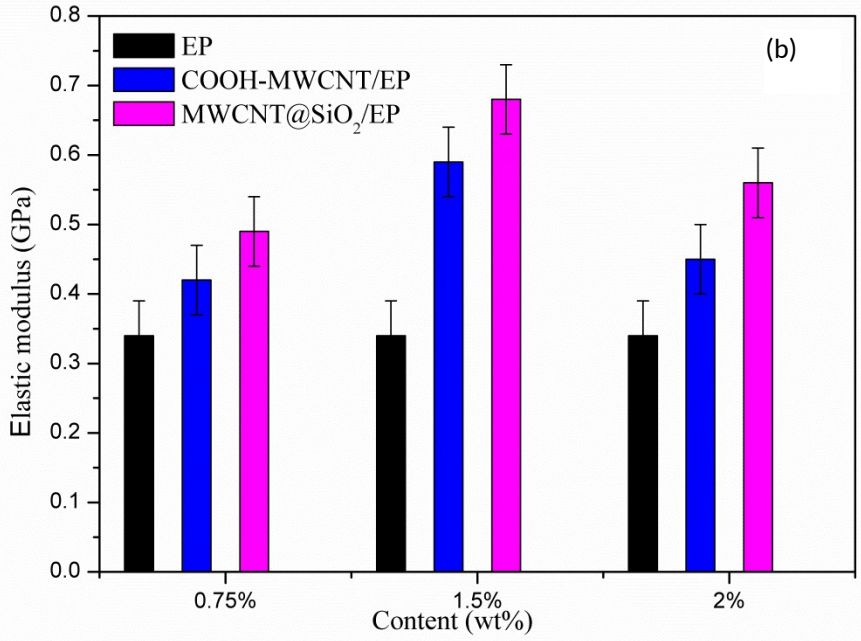
EP
COOH-MWCNT/EP
MWCNT@SiO2/EP
(b)
Elastic modulus (GPa)
0.0
0.1
0.2
0.3
0.4
0.5
0.6
0.7
0.8
0.75%
1.5%
2%
Content (wt%)

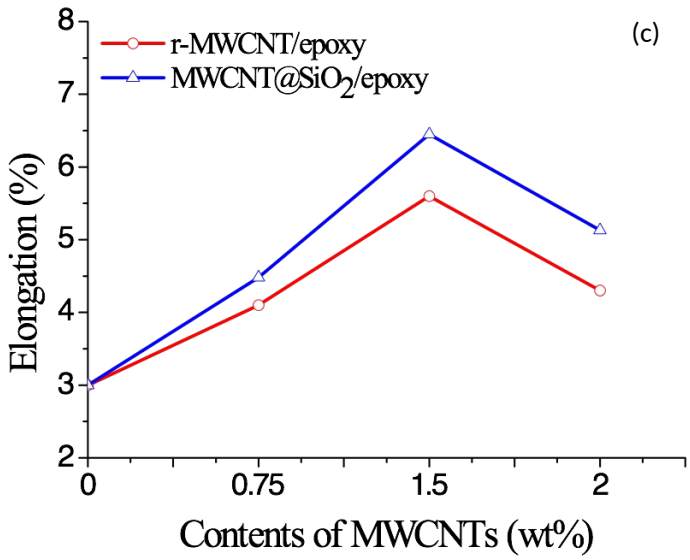

Fig. 9 Mechanical properties of epoxy composites as a function of MWCNTs contents for epoxy composites.